Radiation Detection Technology and Methods manuscript No.
(will be inserted by the editor)

Optimization of multi-reflection time-of-flight mass analyzer operating in in-trap-lift mode

Wen-Xue Huang · Yu-Lin Tian · Yong-Sheng Wang · Jun-Ying Wang · Xiao-Hong Zhou

Received: date / Accepted: date

Abstract *Purpose:* We are building an MRTOF-MS (Multi-Reflection Time-Of-Flight Mass Spectrometer) for isobaric separation for the Lanzhou Penning Trap. The potentials applied on the electrodes of our MRTOF mass analyzer operating in in-trap-lift mode have to be optimized to achieve a very high mass resolving power.

Methods: Our method to design and optimize an MRTOF mass analyzer has been updated to introduce constraints on the potentials and this method now can be used to optimize the parameters of MRTOF-MS both operating in mirror-switching mode and in in-trap-lift mode. By using this method, the optimal potential parameters of the electrodes have been obtained for our MRTOF mass analyzer operating in the in-trap-lift mode.

Results and Conclusion: With a beam size of 2.8 mm diameter and an initial average ion kinetic energy of 1500 eV, the maximal mass resolving power has been achieved to be 3.2×10^4 with a total TOF of 7.0 ms for an ion species of $^{40}Ar^{1+}$. It can reach up to 5.6×10^4 for a beam size of 0.3 mm diameter. The simulation shows that the inaccuracy of the potentials applied on the outermost mirror electrodes M1-M2 must be less than 50 ppm or preferably 20 ppm.

Keywords Time-of-flight mass spectrometer · Multiple-reflection · Mass measurement · Isobaric separation · Exotic nuclei

Supported by the National Natural Science Foundation of China (Grant Nos: 11675224, 11405243, 11605268, 11735017), the Chinese Academy of Sciences (No. 113462KYSB20150026, QYZDJ-SSW-SLH041), and the National Basic Research Program of China (973 Program) (No. 2013CB834400).

W.X. Huang · Y.L. Tian · Y.S. Wang · J.Y. Wang · X.H. Zhou
Institute of Modern Physics, Chinese Academy of Sciences, Lanzhou 730000, China
Tel.: +86-931-4969326
E-mail: huangwx@impcas.ac.cn
ORCID: 0000-0002-3134-5509

Y.L. Tian · Y.S. Wang
School of Physical Sciences, University of Chinese Academy of Sciences, Beijing 100049, China

Y.S. Wang
School of Nuclear Science and Technology, Lanzhou University, Lanzhou 730000, China

1 Introduction

The Multi-Reflection Time-Of-Flight Mass Spectrometer (MRTOF-MS) has been developed as a new device in recent years. By extending the flight path using multi-reflection between electrostatic ion mirrors, an MRTOF-MS can reach a very high mass resolving power of >100,000 in a compact structure. Moreover, it also has other unique advantages, such as extremely short measurement time, a large mass range, very high sensitivity and non-scanning operation. Plaß et al. [1] reviewed the MRTOF-MS developments for the research with short-lived nuclei and different instrumental implementations. Up to now, many MRTOF-MSs for mass measurements and isobaric separations have been commissioned [2–6] or under construction [7–11]. Many good results have been achieved, as examples, the masses of ^{82}Zn [12], ^{53,54}Ca [13] and ^{52,53}K [14] have been measured by using MRTOF-MS at ISOLDE/CERN and the masses of heavy nuclides produced by fusion-evaporation reactions at GARIS-II/RIKEN [15].

Injection and ejection of ions into/from MRTOF-MS have been achieved by switching the electric potentials of the electrodes to appropriate values while

the ions are passing. Thus, according to the switching mode, all MRTOF-MSs can be cataloged into two types: mirror-switching and in-trap-lift modes. In the former mode, the electric potentials of the entrance and exit mirrors are switched to lower values and the potential of the intermediate drift-tube keeps at 0, while in the latter, all the potentials of the mirrors keep at their optimal values and the intermediate drift-tube is switched to its appropriate value, in other words, the drift-tube acts as a lift to the ions and the energies of the ions vary, thus the ions can be injected, trapped and ejected by only switching the potential of the drift-tube. Wolf et al. [16] gave a detail theoretical study, and many MRTOF-MSs [4,6,10] have adopted the in-trap-lift mode.

The Lanzhou Penning Trap (LPT) [17], of which the main task is to perform direct mass measurements on atoms and nuclei with high precision, is presently under construction at the Institute of Modern Physics, Chinese Academy of Sciences. We are building an MRTOF-MS for isobaric separation for LPT. The design and optimization procedures have been reported in detail in Ref. [7,18], where the mirror-switching mode has been assumed and a maximal resolving power has been achieved to be 1.3×10^5 with a total time-of-flight of 6.5 ms for an ion species of $^{40}Ar^{1+}$. In this paper, we report the optimization of our MRTOF mass analyzer operating in in-trap-lift mode and the corresponding results.

2 Parameters of the MRTOF mass analyzer

Fig. 1 shows the geometry of our MRTOF mass analyzer. It consists of two identical electrostatic mirrors (each contains a set of four electrodes) in combination with two einzel lens and a drift-tube. All electrodes of this analyzer have a cylindrical shape. The total length is 708 mm with an inner diameter of 60 mm. The mirror electrodes M1-M4 (numbered from the outermost) have lengths of 20, 16, 26 and 26 mm, respectively, and the lens electrode L has 46 mm. The intermediate drift-tube D has a length of 400 mm. The distance between two adjacent electrodes is 4 mm. The time focus plane where places a micro-channel-plate detector or a Bradbury-Nielsen gate [19] is set to locate 255 mm after the analyzer. Different from our previous optimization, we set the mass analyzer operating in the in-trap-lift mode.

3 Update of the optimization procedure

In our previous paper [7], we reported an optimization strategy in detail to find the optimal parameters for our

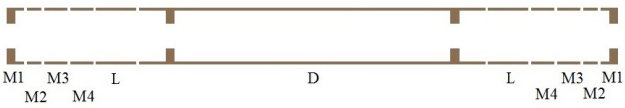

Fig. 1 The geometry of our MRTOF mass analyzer.

mass analyzer operating in the mirror-switching mode. It includes two sub-procedures, a global search and a local refinement. The ion trajectories are calculated in the SIMION [20] according to our specified user program as usual, and the variations of the parameters are performed in a separate optimization program that is coded by ourselves by using the Nelder-Mead simplex algorithm [21]. Because we search all the possibilities in the whole parameter space the best parameters can be found for sure.

We found the drawback of our optimization program when we tried to optimize our MRTOF mass analyzer operating in the in-trap-lift mode. Practically, the kinetic energy of the ions from the RFQ cooler and buncher in the upstream has to be fixed at a certain value, say, 1500 eV. It constrains all the potentials applied on the electrodes of the mass analyzer at <1500 V. Thus, the optimization has to be done according to boundaries on the possible potentials on the electrodes. Our previous program cannot do this and we have to update it.

The Nelder-Mead simplex algorithm originally does not support constraints (upper and lower boundaries). A penalty function or a domain transformation was proposed to use. Box [22] proposed a way to handle some explicit and some implicit constraints and Guin [23] later refined the idea. Le Floc'h [24] compared all these methods. To solve our problem, we perform the following strategy. When a trial point is out of the boundaries and the centroid's coordinate $\overline{P_i}$ respects the constraints, the point is reset at $l + w(\overline{P_i} - l)$ if the lower boundary l is broken or at $h - w(\overline{P_i} - l)$ if the upper boundary h is broken, where w is a uniform random number between 0.00001 and 0.5. If the centroid breaks the constraints, the point is reset at $l + 0.00001$ if the lower boundary is broken or at $h - 0.00001$ if the upper boundary is broken.

4 Results and discussion

To calculate the mass resolving power with respect to the number of revolutions, we considered the following as the initial beam conditions. The beam consists of 100 ions of $^{40}Ar^{1+}$, of which the average kinetic energy is 1500 eV, and the bunch width is 20 ns (FWHM) at the middle of the analyzer. (Since the calculation

is very time-consuming we cannot increase the number of ions due to our existing computation capacity.) In the middle between the ion mirrors the ion beam coordinates x and y orthogonal to the optical axis z, the angles α=dx/dz and β=dy/dz with respect to the axis z and the energy K are approximately represented by Gaussian distributions with the standard deviations σ_x=σ_y=1.0 mm, σ_α=σ_β=1.5 mrad and σ_K=8.5 eV. All these parameters are the same as those in Ref. [7]. For comparison, we also reduce the beam spot from σ_x=σ_y=1.0 mm to 0.5, and 0.1 mm, corresponding to beam sizes with diameters of 2.8, 1.4 and 0.3 mm, respectively. If not specified, the results are obtained for the beam size with 2.8 mm diameter.

The mass resolving power R, which is one of the most important quantities in mass spectrometry, is calculated as $R = TOF/2/\Delta TOF$, where TOF and the overall spread ΔTOF are the centroid and the full-width-at-half-maximum (FWHM) of the time-of-flight peak.

4.1 Optimized results for the beam size with 2.8 mm diameter

Considering the symmetric shape of our MRTOF mass analyzer and the practical potential controls through the power supplies during the experiments, we set the potentials applied on the four mirror electrodes, one lens electrode and the intermediate drift-tube as the optimization parameters, six in total. Because the incoming ions have an average energy of 1500 eV, all the potentials applied on the electrodes have been set an upper limit of 1400 V.

In the global search step, we totally considered $4 \times 4 \times 4 \times 7 \times 9 \times 3 = 12096$ potential combinations as the initial parameter sets and at last chose only the best five new sets obtained from the search for further local refinement. By the Nelder-Mead simplex algorithm all parameters varied and a large number of local minima were obtained. We chose the parameter set which gives the biggest value of mass resolving power as the optimal one, rather than the smallest peak width of the TOF when the mass analyzer operates in the mirror-switching mode; because in the in-trap-lift mode the average kinetic energy of the ions travelling in the trap varies according to the formula, $K_{intrap} = e[1500 - U_{drift}]$, where U_{drift} is the potential of the drift tube, and the total TOF varies with different parameter set.

We optimized the potentials for different number of revolutions and obtained the maximal resolving power that can be achieved, as shown in Fig. 2. For the beam size with 2.8 mm diameter, when increasing the number of revolutions N the maximal resolving power increases steadily and then reaches its maximum around $N \sim 150$. That means, we can get a very good separation of ions in only 3 ms for $^{40}Ar^{1+}$.

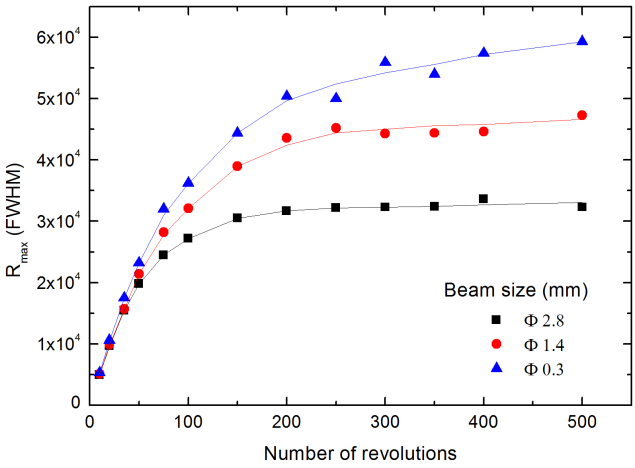

Fig. 2 The maximal mass resolving powerR_{max} achieved at different number of revolutions and different beam size. The lines are to guide the eye.

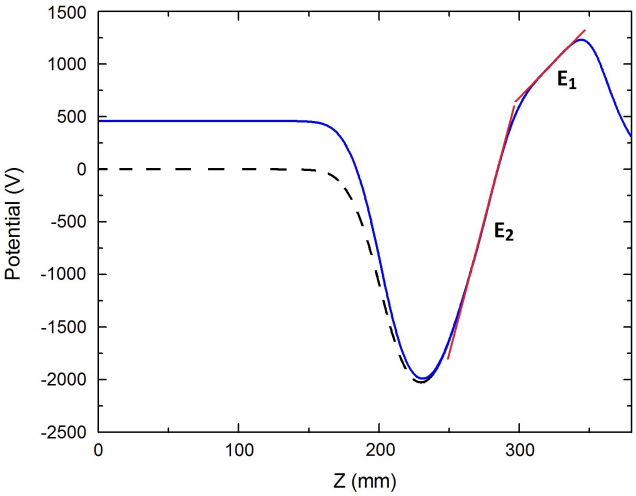

Fig. 3 Potential distribution at the optical axis z in one of the mirrors of the MRTOF mass analyzer for the average ion kinetic energy of 1500 eV. The position $z = 0$ corresponds to the middle point between the ion mirrors. E_1 and E_2 are two regions with approximately constant electric fields. The solid and dash lines correspond to the potential distributions when the ions are injected-into/ejected-from the analyzer and are trapped inside, respectively.

For every optimization for a specific number of revolutions we obtained one potential set with the highest mass resolving power. Table 1 lists the potentials optimized for the number of revolutions of N=350. Fig. 3 shows the potential distribution along the optical axis in one of the mirrors of the analyzer when the ions are injected-into/ejected-from the analyzer and are trapped inside. It has two regions with approximately constant

Table 1 Optimized potentials on the electrodes for the ion species of $^{40}Ar^{1+}$. M1 – M4: mirror electrodes 1 – 4 from outside to inside, L: lens electrode, D: drift-tube.

Electrode	M1	M2	M3	M4	L	D
Potential (V)	1373.4	867.9	962.1	−1046.2	−2436.7	459.8

electric fields [25,26], $E_1 < E_2$. The ions turn around in the weaker constant electric field E_1.

Applying the potentials in Table 1 to the electrodes, we calculated the temporal width at the detector plane with respect to the number of revolutions. Fig. 4 shows the calculation results of the total TOF, the temporal width ΔTOF, and the mass resolving power R as function of number of revolutions. Increasing the number of revolutions, the total time-of-flight almost increases linearly, and the initially high temporal spread decreases until a minimum, only 61 ns at the number of revolutions of $N \sim 100$, and then increases. The maximal resolving power $R = 3.2 \times 10^4$ are achieved at 350 laps, corresponding to a TOF of 7.0 ms.

4.2 Effects of potential inaccuracy

Fig. 5 shows the relative variation of TOF and mass resolving power as functions of relative variation of bias potentials as determined by our optimization code. For the total TOF, the behavior from the mirror electrode M3 acts differently from other electrodes, and the largest variation is from the mirror electrode M1. The maximal achievable mass resolving power decreases as the potentials applied on the electrodes vary from the ideal ones as expected. Except M1 and M2, the potential variations from all other electrodes (M3, M4, L and D) almost have no effect on the final resolving power. Those from the mirror electrode M1 has the biggest effect, the resolving power decreases 22% from 3.2×10^4 to 2.5×10^4 as the relative variation of the potential by 500 ppm. Thus we have to assure the inaccuracy of the potentials applied to the mirror electrodes M1 and M2 to be less than 50 ppm or preferably 20 ppm. It is very easy to understand that the potentials on the electrodes M1 and M2 form the mirrors and the ions turn around at the position between M1 and M2.

4.3 Effects of different beam size

Fig. 2 also shows the maximal mass resolving power achieved at different beam sizes. For the same number of resolutions, we keep all the parameters of the initial beam conditions except the beam size. For all three beam sizes, the maximal resolving powers increase steadily and then reach their maxima as increasing the number of revolutions, but the reaching point delays from $N \sim 150$ to ~ 200 and ~ 300 for the beam size reducing from Φ2.8 mm to Φ1.4 mm and Φ0.3 mm, respectively.

For different beam size, the maximal resolving power increases as the beam size reduces. It reaches 3.2×10^4 for beam size of Φ2.8 mm, increases to 4.4×10^4 for Φ1.4 mm, and to 5.6×10^4 for Φ0.3 mm. The smaller beam size benefits the resolving power, thus we should inject ion beam with a smaller beam size into the mass analyzer to achieve a higher mass resolving power.

4.4 Comparison between the mirror-switching and the in-trap-lift modes

Since we have obtained the optimal parameters for the same mass analyzer operating both in the mirror-switching and the in-trap-lift modes, we can compare them directly. In our optimization, we used the same initial beam conditions described above, the initial beam size is 2.8 mm diameter and the initial average kinetic energy of the ions is 1500 eV. The outcome differences only come from the different operating mode.

In the mirror-switching mode, the maximal resolving power has been achieved to be 1.3×10^5 with a total time-of-flight of 6.5 ms for the ion species of $^{40}Ar^{1+}$; but in the in-trap-lift mode, it is only 3.2×10^4 with a total time-of-flight of 7.0 ms. It seems that the mirror-switching mode is much better than the in-trap-lift mode if we ignore the financial costs of the power supplies and the switches to switch the potentials applied on the different electrodes. The difference in mass resolving power may come from the difference of the kinetic energy of the ions travelling in the trap, which is 1500 eV in the mirror-switching mode and 1040 eV in the in-trap-lift mode in our case. We may promote the mass resolving power in the in-trap-lift mode by increasing the kinetic energy of the ions in the trap. A paper about the relationship between maximal resolving power, kinetic energy in the trap, mass of ion species, beam size, and so on will be prepared after more very time-consuming calculations.

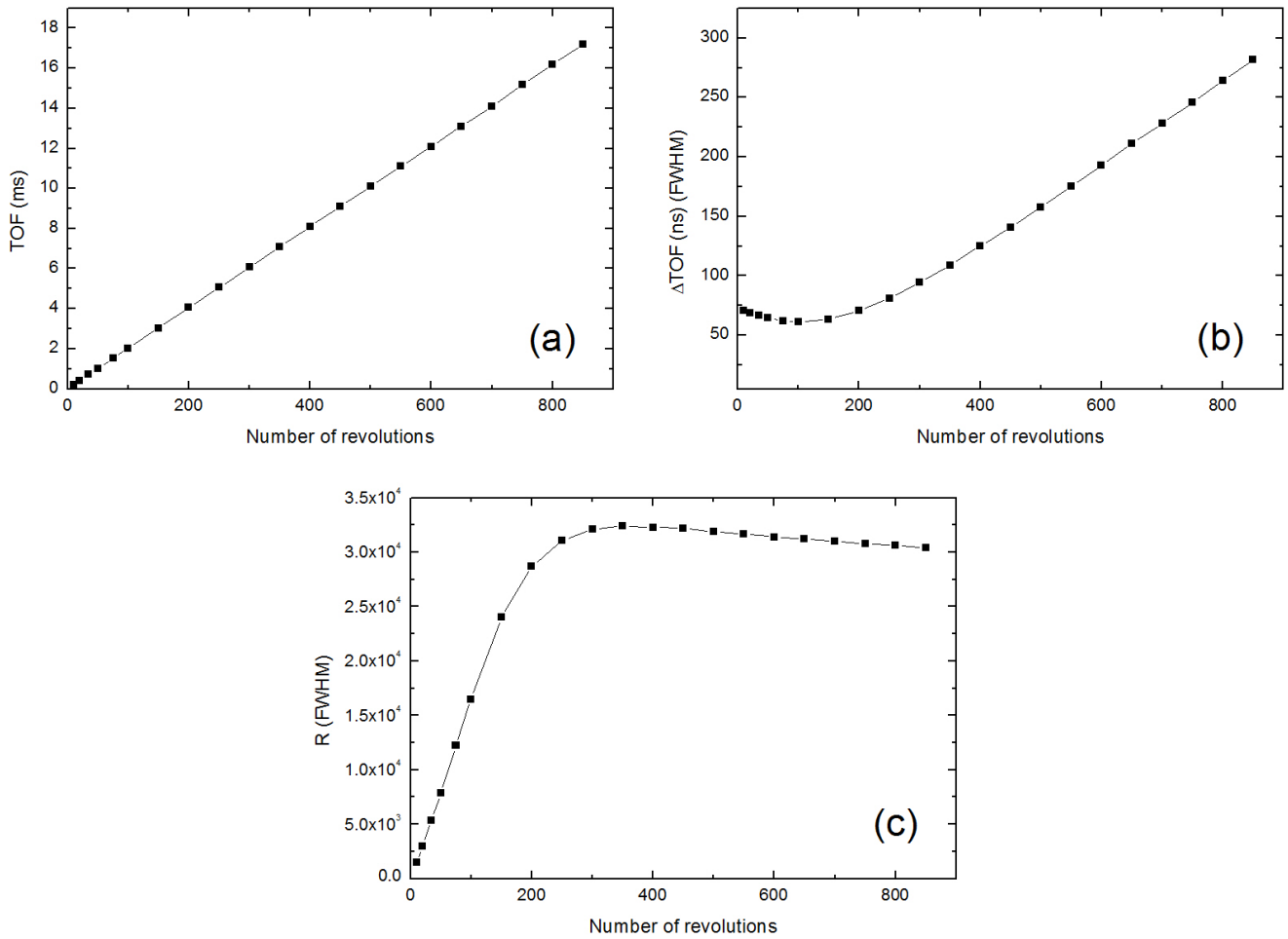

Fig. 4 Calculated results of the TOF (a), the temporal width ΔTOF (b), and the mass resolving power R (c) as function of number of revolutions.

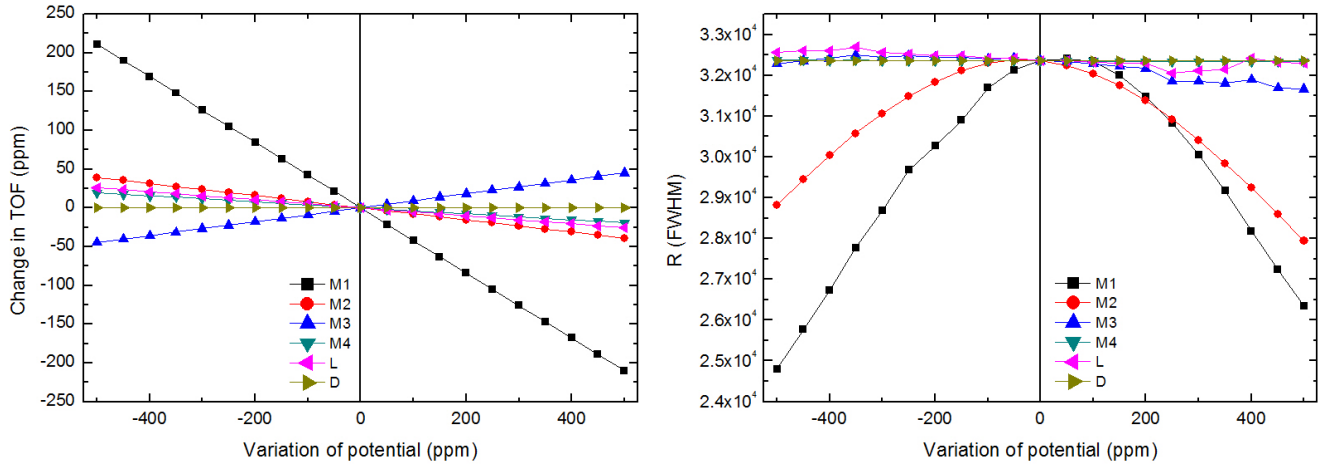

Fig. 5 Calculated relative variation of TOF (left) and mass resolving power R (right) as functions of relative variation of bias potentials as determined by optimization code. M1 – M4: mirror electrodes 1 – 4 from outside to inside, L: lens electrode, D: drift-tube.

5 Summary

Our previous method to design a multiple-reflection time-of-flight mass analyzer has been updated. Now constraints can be applied on the potentials. The method can be used to search the optimal potentials applied on the electrodes in the MRTOF mass analyzer operating not only in the mirror-switching mode but also in the in-trap-lift mode.

By using this updated method, the potentials applied on the electrodes of our MRTOF mass analyzer operating in the in-trap-lift mode have been searched and optimized. With a beam size of 2.8 mm diameter and an initial average ion kinetic energy of 1500 eV, the maximal mass resolving power has been achieved to be 3.2×10^4 with a total time-of-flight of 7.0 ms for an ion species of $^{40}Ar^{1+}$. The maximal resolving power can reach up to 5.6×10^4 for a beam size of 0.3 mm diameter. The simulation also shows that the variations of the potentials applied to the mirror electrodes M3-M4, the lens electrode L and the drift-tube D almost have no effect on the final resolving power. Crucially, the inaccuracy of the potentials on the mirror electrodes M1-M2 needs to be less than 50 ppm or preferably 20 ppm.

References

1. W. R. Plaß, T. Dickel, C. Scheidenberger, Multiple-reflection time-of-flight mass spectrometry, Int. J. Mass Spectrom. 349-350, 134-144 (2013).
2. A. Piechaczek, V. Shchepunov, H. K. Carter, et al., Development of a high resolution isobar separator for study of exotic decays, Nucl. Instrum. Methods Phys. Res. Sect. B 266, 4510-4514 (2008).
3. P. Schury, K. Okada, S. Shchepunov, et al., Multi-reflection time-of-flight mass spectrograph for short-lived radioactive ions, Eur. Phys. J. A 42, 343-349 (2009).
4. R. N. Wolf, F. Wienholtz, D. Atanasov, et al., ISOLTRAP's multi-reflection time-of-flight mass separator/spectrometer, Int. J. Mass Spectrom. 349-350, 123-133 (2013).
5. W. R. Plaß, T. Dickel, U. Czok, et al., Isobar separation by time-of-flight mass spectrometry for low-energy radioactive ion beam facilities, Nucl. Instrum. Methods Phys. Res. Sect. B 266, 4560-4564 (2008).
6. T. Y. Hirsh, N. Paul, M. Burkey, et al., First operation and mass separation with the CARIBU MR-TOF, Nucl. Instrum. Methods Phys. Res. Sect. B 376, 229-232 (2016).
7. Y. L. Tian, Y. S. Wang, J. Y. Wang, X. H. Zhou, W. X. Huang, Designing a multi-reflection time-of-flight mass analyzer for LPT, Int. J. Mass Spectrom. 408, 28-32 (2016).
8. J. W. Yoon, Y.-H. Park, S. J. Park, G. D. Kim, Y. K. Kim, Design of the multi-reflection time-of-flight mass spectrometer for the RAON facility, EPJ Web Conf. 66, 11042 (2014).
9. B. E. Schultz, J. M. Kelly, C. Nicoloff, J. Long, S. Ryan, M. Brodeur, Construction and simulation of a multi-reflection time-of-flight mass spectrometer at the University of Notre Dame, Nucl. Instrum. Methods Phys. Res. Sect. B 376, 251-255 (2016).
10. P. Chauveau, P. Delahaye, G. De France, et al., PILGRIM, a multi-reflection time-of-flight mass spectrometer for Spiral2-S3 at GANIL, Nucl. Instrum. Methods Phys. Res. Sect. B 376, 211-215 (2016).
11. C. Jesch, T. Dickel, W. R. Plaß, et al., The MR-TOF-MS isobar separator for the TITAN facility at TRIUMF, Hyperfine Interact. 235, 97-106 (2015).
12. R. N. Wolf, D. Beck, K. Blaum, et al., Plumbing neutron stars to new depth with the binding energy of the exotic nuclide ^{82}Zn, Phys. Rev. Lett. 110, 041101 (2013).
13. F. Wienholtz, D. Beck, K. Blaum, et al., Masses of exotic calcium isotopes pin down nuclear forces, Nature 498, 346-349 (2013).
14. M. Rosenbusch, P. Ascher, D. Atanasov, et al., Probing the $N = 32$ Shell Closure below the Magic Proton Number $Z = 20$: Mass Measurements of the Exotic Isotopes $^{52,53}K$, Phys. Rev. Lett. 114, 202501 (2015).
15. P. Schury, M. Wada, Y. Ito, et al., First online multi-reflection time-of-flight mass measurements of isobar chains produced by fusion-evaporation reactions: Toward identification of superheavy elements via mass spectroscopy, Phys. Rev. C 95, 011305 (2017).
16. R. N. Wolf, G. Marx, M. Rosenbusch, L. Schweikhard, Static-mirror ion capture and time focusing for electrostatic ion-beam traps and multi-reflection time-of-flight mass analyzers by use of an in-trap potential lift, Int. J. Mass Spectrom. 313, 8-14 (2012).
17. W. X. Huang, Y. L. Tian, J. Y. Wang, et al., Status of Lanzhou Penning Trap for accurate mass measurements, Nucl. Instrum. Methods Phys. Res. Sect. B 317, 528-531 (2013).
18. Y. S. Wang, Y. L. Tian, J. Y. Wang, X. H. Zhou, W. X. Huang, Design and optimization of a multi-reflection time-of-fight mass spectrometer for LPT, Nucl. Phys. Rev. 34, 624-629 (2017). (in Chinese)
19. N. E. Bradbury, R. A. Nielsen, Absolute values of the electron mobility in hydrogen, Phys. Rev. 49, 388-393 (1936).
20. D. J. Manura, D. A. Dahl, SIMION 8.0/8.1 User Manual, Scientific Instrument Services, Inc., Idaho National Laboratory (2011).
21. J. Nelder, R. Mead, A simplex method for function minimization, Comput. J. 7, 308 (1965).
22. M. J. Box, A New Method of Constrained Optimization and a Comparison With Other Methods, Comput. J. 8, 42-52 (1965).
23. J. A. Guin, Modification of the Complex Method of Constrained Optimization, Comput. J. 10, 416-417 (1968).
24. F. Le Floc'h, Issues of Nelder-Mead simplex optimisation with constraints, January 2, 2012. Available at http://dx.doi.org/10.2139/ssrn.2097904.
25. H. Wollnik, A. Casares, An energy-isochronous multi-pass time-of-flight mass spectrometer consisting of two coaxial electrostatic mirrors, Int. J. Mass Spectrom. 227, 217-222 (2003).
26. B. A. Mamyrin, V. I. Karataev, D. V. Shmikk, V. A. Zagulin, The mass-reflectron, a new nonmagnetic time-of-flight mass spectrometer with high resolution, Sov. Phys. JETP 37, 45-48 (1973).